EVALUATING THE PERFORMANCE OF FIBER-BASED CONCRETE MIXES FOR VARIOUS APPLICATIONS

Submitted to

Stewart Kriegstein, Managing Member

stewart@warstoneinnovations.com

Warstone Innovations, LLC, 1622 Walter St, Suite A, Ventura, CA 93003

By

Surya S. C. Congress, PhD
Assistant Professor, Michigan State University

Krishneswar Ramineni,
Doctoral Student, Texas A&M University (TAMU)

Anand J. Puppala, PhD, PE, BC.GE, F-ICE, Dist. M. ASCE

Professor | A.P. and Florence Wiley Chair, Texas A&M University (TAMU)

NSF Industry University Cooperative Research Center (IUCRC) Site at TAMU

Zachry Department of Civil and Environmental Engineering

Texas A&M University (TAMU), Room: 801 A&B, Dwight Look Engineering Building (DLEB)

College Station, TX 77843-3136

Email: anandp@tamu.edu

GRAPHICAL ABSTRACT

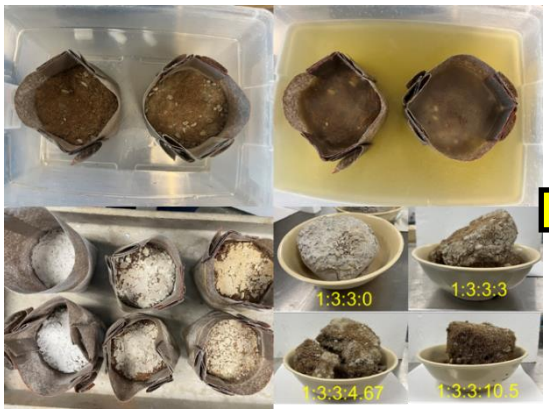

Small-scale and large-scale lab wetting and drying (Durability) tests on fiber-based concrete mixtures

Fiber-based concrete mixture for flooding and erosion protection applications[a]

Strength tests on fiber-based concrete mixtures

Urban and coastal flooding[b]

Potential application to prevent similar scenarios: Mirlo beach after ineffective sandbag protection[c]

Source: [a]Warstone Innovations, LLC, [b]AP Photo/U.S. Air Force, Master Sgt. Mark C. Olsen, and [c]Dare county- NCDOT

ABSTRACT

Rising seawater levels and increased frequency of storms due to climate change cause flooding, coastal erosion, and water pollution. These not only impact coastal communities and infrastructure but also pose challenges to the recovery of the communities. Sandbag barriers are traditionally used to control the destructive behavior of flooding and stormwater. The resistance generated by sandbags depends on the gravity of these bags. The number of sandbag barriers needed to protect the assets depends on the impact of the hydraulic forces of the runoff water and the debris flowing in the storm. Moreover, sandbags deteriorate when they are exposed to prolonged wetting and drying cycles. The current study identified the need to improve the performance of these barriers by adopting a relatively lightweight and durable mix with water absorption characteristics to counter the handling and transportation costs and extend the service life. This research evaluated the durability of various fiber-based concrete mixtures with different fiber percentages (0%, 30%, 40%, 50%, and 60% by volume of the mixture). Further, the influence of fiber dosage on free swell strain, permeability, water absorption/desorption, and compressive and tensile strength properties of the fiber-based concrete mixes was evaluated. Permeability increased with higher fiber dosages, resulting in a more porous structure. The absorption and desorption tests showed that fiber-based mixtures reach equilibrium within 48 hours, with negligible weight changes thereafter. The strength tests conducted by previous literature used mixes having a fraction of the highest fiber mixture considered in this study. Hence, the applicability of the traditional strength testing was ambiguous and needs further studies to establish a reliable protocol. The study concluded that fiber-based concrete mixes can be promising alternatives to sandbags in flood control applications due to their high permeability and water absorption properties. Further research is required to optimize fiber dosage and mix proportions to enhance strength and sustainability properties for potential new applications.

ACKNOWLEDGEMENTS

This research was funded by Warstone Innovations, LLC. (Stewart Kriegstein) as a part of the National Science Foundation's (NSF) Industry-University Cooperative Research Center (I/UCRC)'s 'Center for Integration of Composites into Infrastructure (CICI)' site at TAMU. The authors would like to acknowledge the help of Dr. Nripojyoti Biswas, Akash Ashok Tanshette, and Nicole Arackal for their help in conducting large-scale wetting and drying tests. The authors would also like to acknowledge other members of Dr. Puppala's Infrastructure Research Group at TAMU for their support and help in various phases of the research.

The authors would also like to acknowledge the financial support of NSF towards the I/UCRC CICI site at TAMU (NSF PD: Dr. Prakash Balan; Award #2017796). Any findings, conclusions, or recommendations expressed in this material are those of the authors and do not necessarily reflect the views of the National Science Foundation.

TABLE OF CONTENTS

LIST OF FIGURES

LIST OF TABLES

1. INTRODUCTION

1.1. Background

In recent decades, climate change has become a huge global concern. The changing sea levels and increased frequency and intensity of storms due to climate change are affecting human activities and infrastructure in coastal areas. Rising sea levels make coastal areas vulnerable to coastal flooding, shoreline erosion, water pollution, and an increase in the salinity of coastal waters (Environmental Protection Agency, 2016). Frequent coastal flooding can have a huge impact on coastal communities and make coastal infrastructure vulnerable to storm surges and exposure to saline water. According to recent statistics, over 8.6 million Americans live in areas susceptible to coastal flooding and more than $1 trillion of property and infrastructure is at risk of frequent inundation (Bradford, 2016; Wuebbles et al., 2017). There have been many flood protection solutions developed over time to prevent the impact of flooding.

1.2. Problem Statement

Traditional flood protection solutions such as concrete seawalls, sandbag barriers, and levees, while effective, are associated with high financial costs, environmental disruption, and resource-intensive construction processes. Sandbagging, a common technique, faces significant challenges including labor-intensive deployment, logistical issues, and limited effectiveness in flash flood scenarios. Alternative solutions like sandbag replacement systems (SBRS) and hydrogels, although innovative, require substantial initial investments and present practical limitations, particularly in coastal environments (Gorman, 2020; Kevin Biggar & Srboljub Masala, 1998; Lankenau et al., 2020; Lankenau & Koppe, 2019; Massolle et al., 2018). To address these challenges, there is a growing interest in sustainable and cost-effective flood control measures leveraging natural materials. Coir, a natural fiber extracted from coconut husks, has demonstrated durability, biodegradability, and high resistance to saltwater, making it an ideal candidate for coastal applications. Despite its historical use in erosion control and construction, the potential of coir in cement mixtures for constructing flood barriers remains unexplored.

1.3. Research Objective

The objective of the present experimental study is to evaluate the performance of fiber-based concrete mixes in terms of characteristics that will help address the flooding and erosion-related coastal infrastructure problems caused due to climate change.

1.4. Research Methodology

This study has been divided into four distinct tasks, each aimed at accomplishing the proposed research objective. Figure 1 shows the research flow employed in the current study to achieve the research objective.

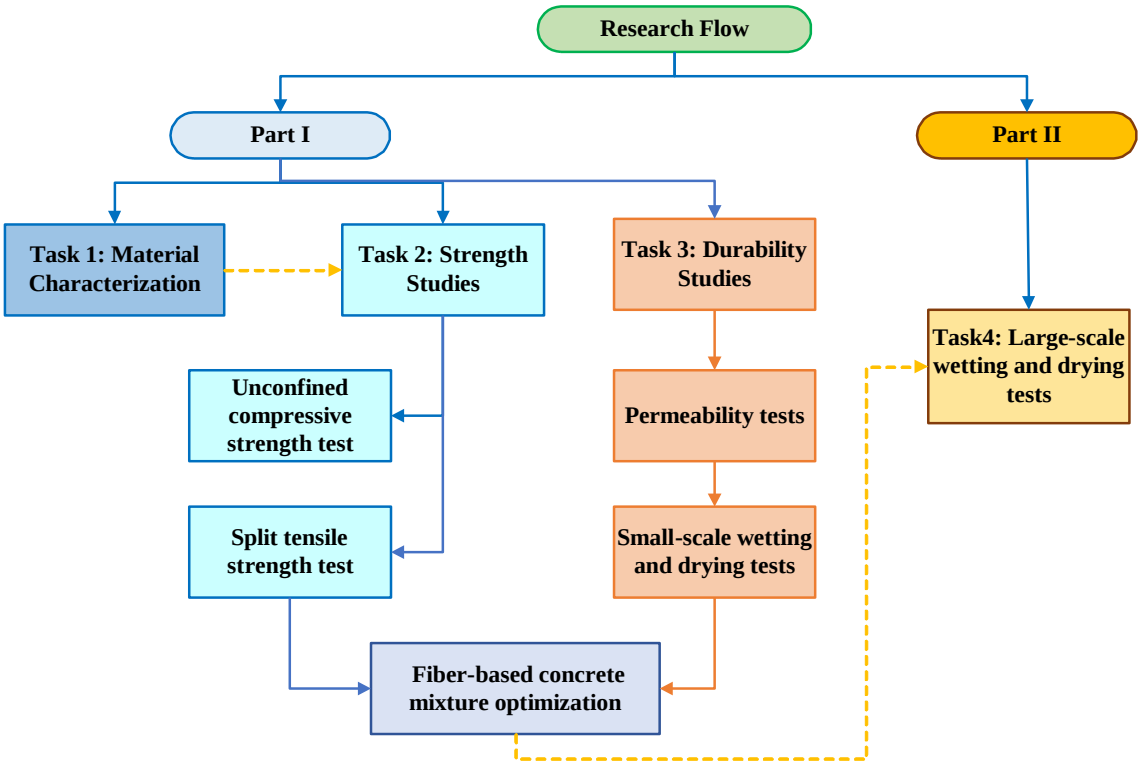

Figure 1. Research flow in the current study

1.5. Report Organization

This report is structured into four chapters. Chapter 1 introduces the problems associated with coastal flooding and erosion control materials, problem statements, research objectives, research methodology, and an overview of the report's organization. Chapter 2 presents a comprehensive literature review on flood control methods and natural fibers in

concrete. Chapter 3 focuses on the experimental work conducted and presents the strength and durability results obtained from the experimental investigation. Finally, Chapter 4 concludes the report by summarizing the test results and presenting recommendations and future scope based on the experimental results.

2. LITERATURE REVIEW

2.1. Background

Coastal and urban flooding present a significant and growing challenge to communities worldwide, driven by various factors such as rising sea levels, increased storm intensity, and climate change impacts on coastal environments (EPA, 2023). Traditional barriers like seawalls, dikes, and levees offer robust protection but often come with environmental trade-offs and high maintenance costs (Wang et al., 2022). Sandbagging has been one of the most popular flood protection techniques used throughout the world. In this method, the bags filled with sand are stacked one over the other to form a wall to prevent flooding (US Army Corps of Engineers, 2012). The walls are constructed in certain patterns to withstand the hydraulic forces of the flood and to take the impact from flood debris. Although this method has been successfully used to prevent flooding, there have always been transportation and handling concerns with this method (Freeman, 2002). The sandbagging method requires a significant amount of time and is labor-intensive, which is not ideal in cases of flash flood situations. Moreover, sand-filled bags deteriorate over time.

To overcome these problems, different sandbag replacement systems (SBRS) like tubes, basin flap, trestle, dam, or panel systems have been developed in the last few decades to control flooding. These SBRSs can be used to make flood protection operations efficient but with a huge initial investment (Kevin Biggar & Srboljub Masala, 1998; Lankenau et al., 2020; Lankenau & Koppe, 2019; Massolle et al., 2018). Moreover, some of the SBRS methods use huge elements that consume space and cause logistical problems. Apart from these, some researchers used hydrogels to develop flood barriers that expand when water is absorbed and collapse as the water dries out (Gorman, 2020). This mechanism helped to overcome transportation and handling issues but its limitations in coastal environments encouraged researchers to explore new techniques and materials in the area of flood-barriers. As the demand for sustainable and cost-effective flood control

measures intensifies, innovative approaches leveraging natural and renewable materials are garnering attention.

2.2. Coir Fiber-Based Concrete Mixtures

One such promising material is coir, a natural fiber extracted from the husk of coconuts, which is abundant in tropical regions. Coir is renowned for its durability, biodegradability, and high resistance to saltwater, making it an ideal candidate for coastal applications (Ahmad et al., 2022). Historically, coir has been employed in a variety of contexts, including erosion control, horticulture, and as a geotextile in construction projects (Ali et al., 2022; Mohammed et al., 2023). Coconut coir is also effectively utilized in flood control through various applications, including coir-based geotextiles, natural coastal defense structures, temporary flood barriers and Coir-based concretes. Coir geotextiles are used for erosion control and slope stabilization, promoting soil retention, vegetation growth, and reducing surface runoff, thereby enhancing the stability of coastal embankments (Meor et al., 2020). Natural coastal defense structures, such as coir logs and rolls, help stabilize shorelines, promote sediment deposition, and support vegetation establishment, mitigating wave energy and storm surge impacts for long-term resilience. Additionally, coir fibers are used to create lightweight, easy-to-deploy, biodegradable temporary flood barriers, offering an environmentally friendly alternative for emergency flood response scenarios (Ali et al., 2022). Over the last two decades, numerous studies have been conducted to understand the durability performance of coir as a potential reinforcement in cement-based materials.

2.2.1. Durability Properties of Coir Fiber-Based Concrete Mixtures

Abdullah, (2011) performed a study on replacing sand with coconut coir and reported that an optimum fiber content of 9% demonstrated better moisture absorption. It also noted that an increase in fiber content correspondingly increased the percentage of water absorption and moisture content. Ramli et al., (2013) investigated the durability properties like chloride and gas permeability of coconut fiber-reinforced concrete under varied environmental conditions. Their findings suggested that using a reduced amount of coconut fiber could enhance durability. They recommended limiting coconut fiber to

approximately 1.2% by volume of cement to ensure optimal long-term durability and strength across various aggressive environments. Koňáková et al., (2015) investigated the use of coir pith, a component of coir, in cementitious composites. They found that a 5% addition of coir pith can enhance the physical properties of concrete, but higher dosages can lead to increased porosity. Chemical treatments of coir pith, such as acetylation or NaOH, were also found to improve the hygric and thermal properties of cementitious composites. This study also reported that moisture content has a significant influence on the thermal properties of coir-based cement mixes. Hwang et al., (2016) investigated the effects of incorporating random, short coconut fibers into various cementitious composites, focusing on rheological properties, mechanical properties, moisture absorption, plastic cracking, and impact resistance. The study found that an increase in dosage of coconut fibers reduced density and necessitated an increase in the superplasticizer dosage for enhanced workability of the fiber-based mixture. Additionally, they reported that higher water-to-binder ratios and higher percentages of fiber led to higher water absorption rates. Martinelli et al., (2023) review on the use of coconut fiber in cement composites highlights that chemical treatment of natural fibers improves adhesion between the cement matrix and fibers through chemical reactions. The study notes that the hydrophilic nature of natural fibers and the hydrophobic nature of matrix result in weak interface bonds, but chemical treatment reduces the fibers' hydrophilicity and enhances adhesion. Additionally, the review concluded that coconut fibers in cement composites. showed better durability properties in terms of water absorption, adhesion, and strength.

2.2.2. Mechanical Properties of Coir Fiber-Based Concrete Mixtures

Hwang et al., (2016) reported that higher water-to-binder ratios were linked to decreased compressive strength. As the ratio of coconut fiber to mortar ranged from 0% to 4%, the 28-day flexural strength of cementitious sheets increased from 5.2 to 7.4 MPa, and the modulus of rupture increased from 6.8 to 8.8 MPa. The increase in coconut fiber dosage by up to 4% had a positive impact on first-crack deflection, toughness indices, plastic cracking behavior, and impact resistance in the composites. Rumbayan & Ticoalu, (2019)

found that the optimum amount of coconut fiber in concrete is 0.25%, which provided approximately 19% improvement in compressive and flexural strength at 28 days. Teixeira et al., (2022) and Katman et al., (2022) reported that the addition of coir fibers to cement-based composites can improve their physical and mechanical properties, with 2% coir fiber modification offering the highest strength.

2.3. Research Direction

These studies collectively suggest that coir-based concrete mixtures, due to their durability and mechanical properties, have the potential to be effective barriers to controlling coastal flooding. Despite numerous studies demonstrating coir's ability to enhance the workability and mechanical properties of coir fiber-based concrete mixtures, research on its durability aspect remains limited. Previous studies have typically restricted the fiber content up to 15%, leaving a gap in understanding the effects of higher dosages of coir fiber in concrete. Additionally, there are no recommendations and testing standards for the usage of higher dosages of coir in concrete mixtures. Investigating the long-term durability of high percentage coir in coir fiber-based concrete mixtures, particularly in flood control barriers under extreme conditions is crucial to ensuring the structural integrity of such materials over time and varying environmental stresses. There is a growing need to assess the properties like absorption and desorption of fiber mixes, which are critical for the performance of fiber-based concrete mixture bags for flood barriers. This study focuses on developing and optimizing high-fiber dosage concrete mixtures, aiming to enhance performance as flood and erosion control devices under extreme conditions.

3. EXPERIMENTAL INVESTIGATION AND RESULTS

3.1. Introduction

This section presents the experimental investigation performed to understand the durability and mechanical behaviors of fiber-based cement mixtures. It provides a brief outline of basic material characterization followed by the experimental tests performed to evaluate the durability and mechanical behavior of fiber-based cement mixtures. At the end of the section, the results and discussion on fiber-based cement mixtures are presented.

3.2. Material Testing and Characterization

The materials used in the present study are Type I ordinary Portland cement, fine, coarse aggregate, natural cut fibers, and geotextile.

3.2.1. Cement

According to ASTM C-150, Type 1 Portland cement was used in the current study. The Blaine fineness of the Portland cement was 378 m^2/kg, and the specific gravity was 3.09. The physical properties of Portland cement are provided in Table 1.

Table 1. Physical Properties of cement

Material Properties	Values	Standards
Air content (Volume %)	9	ASTM C165
Blaine Fineness (m^2/kg) *	378	ASTM C204
Autoclave Expansion (%) *	0.02	ASTM C151
Initial Setting time (minutes)	107	ASTM C191
7 days minimum Compressive strength (MPa)	35.7	ASTM C109
28 days minimum Compressive strength (MPa)	43.9	ASTM C109

*Note: Values obtained from the manufacturer

3.2.2. Aggregates

The locally available river sand was used as the fine aggregate and pea gravel with a maximum size of 12.5 mm was used as coarse aggregate. The particle size gradation for

both fine and coarse aggregates is shown in Figure 2 and the physical properties are shown in Table 2.

Table 2. Physical properties of fine and coarse aggregates

Material properties	Values		Standards
	Fine aggregate	Coarse aggregate	
Specific Gravity, G_s	2.63	2.619	ASTM C127,128
Water Absorption (%)	1.15	0.74	ASTM C127
Dry Rodded Unit Weight (kg/m^3)	1791	1647	ASTM C29

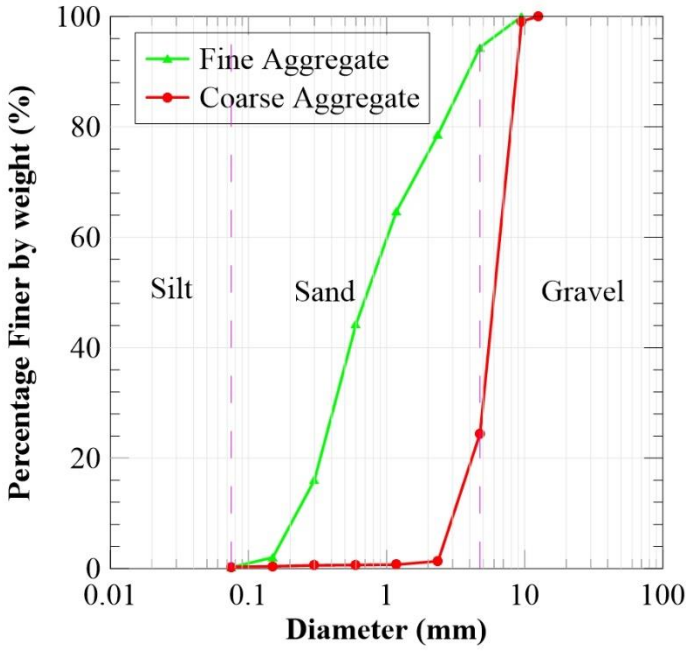

Figure 2. Grain size distribution of fine and coarse aggregates

3.2.3. Fibers

Cut natural coir was used as fibers in the present study. The cut natural coir was prepared by cutting the dry coconut coir into fibers that are 5 to 25 mm long and varying in diameter from 0.25 to 0.3 mm. The water absorption of the cut natural fibers was 300%.

3.2.4. Geotextile

A commercially available nonwoven geotextile that is permeable was used to make cement mixture bags. Figure 3 shows the nonwoven geotextile used in the current study.

Figure 3. Texture of Nonwoven geotextile

3.2.5. Saltwater

The saltwater for the wetting and drying tests was prepared by mixing various salts in specified ratios to replicate seawater composition. The chemical composition of the saltwater prepared is shown in Table 3.

Table 3. Chemical Composition of the saltwater prepared in laboratory

Ionic Constituents	Concentration (gram/kg of solution)
Chloride	19.13
Sodium	10.59
Magnesium	1.07
Calcium	0.54
Potassium	0.52

3.3. Mix Proportions

The mix proportion of fiber-based cement mixtures is shown in Table 4. The mix proportions are denoted in volume parts of cement: fine aggregate: coarse aggregate: fiber. For example, the mix 1:3:3:10.5 in each volume has 1 part of cement: 3 parts of fine aggregate: 3 parts of coarse aggregate and 10.5 parts of cut fibers. The following

nomenclature was used to describe the mixtures based on their specific compositions: mixture I (1:3:3:10.5), mixture V (1:3:3:0), mixture II (1:3:3:7), mixture III (1:3:3:4.67), and mixture IV (1:3:3:3). The mixture constituents used in the study are shown in Figure 4.

Table 4. Mix proportions of fiber-based cement mixtures

Mixture	I	II	III	IV	V
Fiber Percentage	**60%**	**50%**	**40%**	**30%**	**0%**
Mix Proportions	1:3:3:10.5	1:3:3:7	1:3:3:4.67	1:3:3:3	1:3:3:0
Cement (grams)	86.30	107.87	129.41	151.02	215.75
Sand (grams)	322.10	402.63	483.01	563.68	805.25
Pea Gravel (grams)	296.27	370.33	444.27	518.47	740.67
Fiber (grams)	135.92	113.27	90.65	67.96	0.00

Figure 4. Fiber-based concrete mixture constituents

3.4. Experimental Tests

A series of laboratory tests were conducted to evaluate the durability and strength properties of the fiber-based concrete mixtures. The free swell strain test, permeability, and wetting and drying tests were conducted to understand the durability behaviors of the fiber-based concrete mixtures. It should be noted that there are no testing standards and

guidelines established in previous studies to perform tests on high-percentage fiber-based concrete mixtures. The following sections discussed the testing procedures adopted for each test.

3.4.1. Free Swell

The swelling characteristics of fiber-based cement mixtures were investigated using One-Dimensional (1-D) free swell tests. Figure 5 shows the free swell test setup for testing fiber-based cement mixtures. The free swell specimens, with a diameter of 50 mm and a height of 20 mm were prepared using dry fiber-based cement mixture proportions. Free swell tests were performed under a vertical stress of 1 kPa according to the ASTM D4546 method. A linear variable differential transformer (LVDT) recorded the change in height as the specimens were submerged in water. The LVDT readings were taken until there was no change in vertical displacement for three consecutive days.

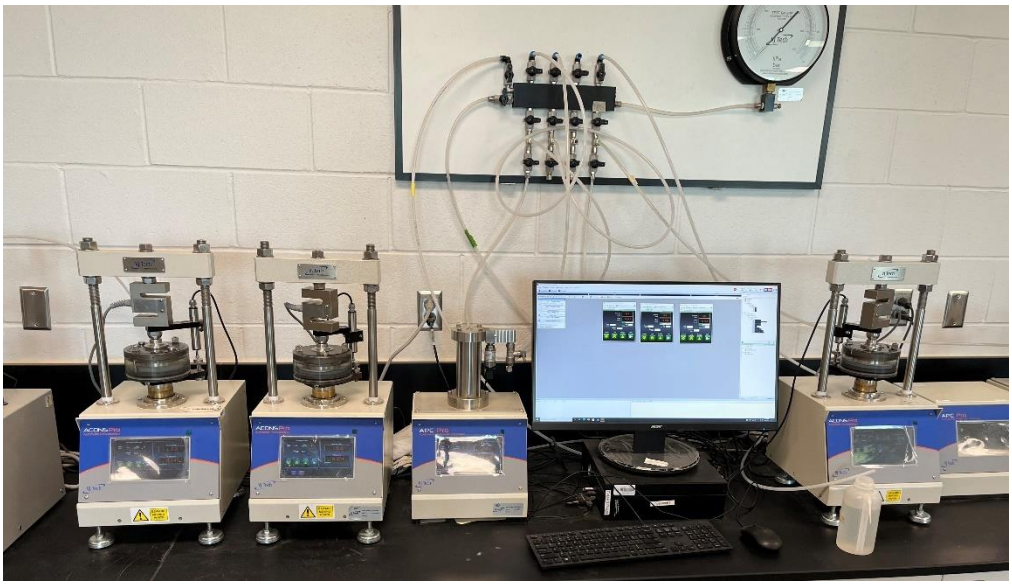

(a)

(b) (c)

Figure 5. Free swell testing a) Test setup b) Specimen before testing c) Specimen after testing

3.4.2. Permeability Tests

The hydraulic conductivity of the fiber-based cement mixtures was measured using a falling head permeability test method. Figure 6a shows the 150 mm diameter and 100 mm height permeability sample preparation and Figure 6b shows the falling head test setup used in the current study to measure the hydraulic conductivity for different fiber-based cement mixes.

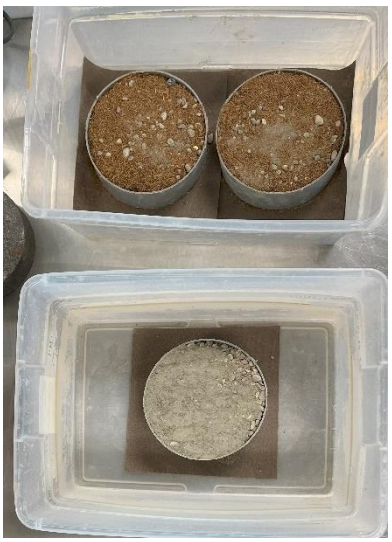

(a) (b)

Figure 6. Permeability Test (a) Sample preparation and (b) Permeability apparatus setup

The specimen was mounted in a permeameter, and the specimen was fully saturated by sending the water from the bottom and collecting it from the top of the specimen. To reduce the water movement through the space between the membrane and the specimen, a 10 kPa confining pressure was applied. The saturation stage was stopped when no air pockets were observed, and the water flow was continuous through the top outlet. The hydraulic conductivity (*k*) of the fiber-based cement mixture was calculated using

$$k_v = 2.303 \times \frac{al}{At} \times \frac{h_1}{h_2} \quad \textbf{(1)}$$

Where, *k* = Hydraulic conductivity, cm/sec

A = Cross section area of the specimen, cm^2

a = Cross section area of the standpipe, cm^2

l = Height of the specimen, cm

h_1 = Water head before the test, cm

h_2 = Water head after the test, cm

3.4.3. Wetting and Drying tests

Wetting and drying tests are essential for understanding and optimizing materials used in flood barriers and erosion control. These tests evaluate how alternating wet and dry conditions affect the stability and durability of materials, which is crucial for ensuring that flood barriers can withstand the forces of water over time. Wetting and drying can significantly alter the hydraulic properties of materials, affecting water absorption, desorption, and permeability. Conducting these tests on fiber-based concrete mixtures evaluates how effective these mixes can be for flood and erosion barrier applications.

3.4.3.1. Small-Scale Tests

A series of wetting and drying tests were conducted on five fiber-based concrete mixtures. 100 × 100 mm wide and 200 mm depth prism-shaped geotextile bags are prepared by

gluing the non-woven geotextile. Different concrete mixture samples of 100 × 100 × 100 mm dimensions were prepared based on the mix proportions. For all concrete mixtures, the constituents were mixed in dry conditions and were placed in geotextile bags. Figure 7 shows various steps involved in the small-scale wetting and drying tests.

The small-scale wetting and drying studies are conducted in two curing conditions: potable water (PW) and saltwater (SW) conditions. The potable water samples were tested in three different simulated environments: 40% relative humidity (RH) and 4°C, 50% RH and 20°C, and 20% RH and 40°C. In contrast, the saltwater samples were tested in two different temperatures: one set in 50% RH and 20°C for both wetting and drying and another set in 40 % RH and 4°C for wetting cycles and 50% RH and 20°C for drying cycles. The nomenclature of Temperature-Relative Humidity-Curing conditions was adopted in the report. For example, 4°C-40RH-PW indicates the testing was performed at 4°C temperature and relative humidity of 40% by immersing in potable water.

A total of five wetting and drying cycles were performed on each mixture except for samples tested under 4°C-40RH-PW conditions. The first wetting cycle of all mixes was conducted by completely immersing the dry cement mixture bags in water, and weights were recorded every 24 hours until the sample reached a constant mass. After retrieving the cement mixtures from the water bath, the drying cycle was conducted by placing them in a controlled environment room maintained at the specified relative humidity and temperature conditions. Similar to the wetting cycle, the weights of the drying specimens were recorded every 24 hours until the weight change was negligible. In the current testing, any weight change of less than one percent over 24 hours was considered negligible and the sample is assumed to attain equilibrium.

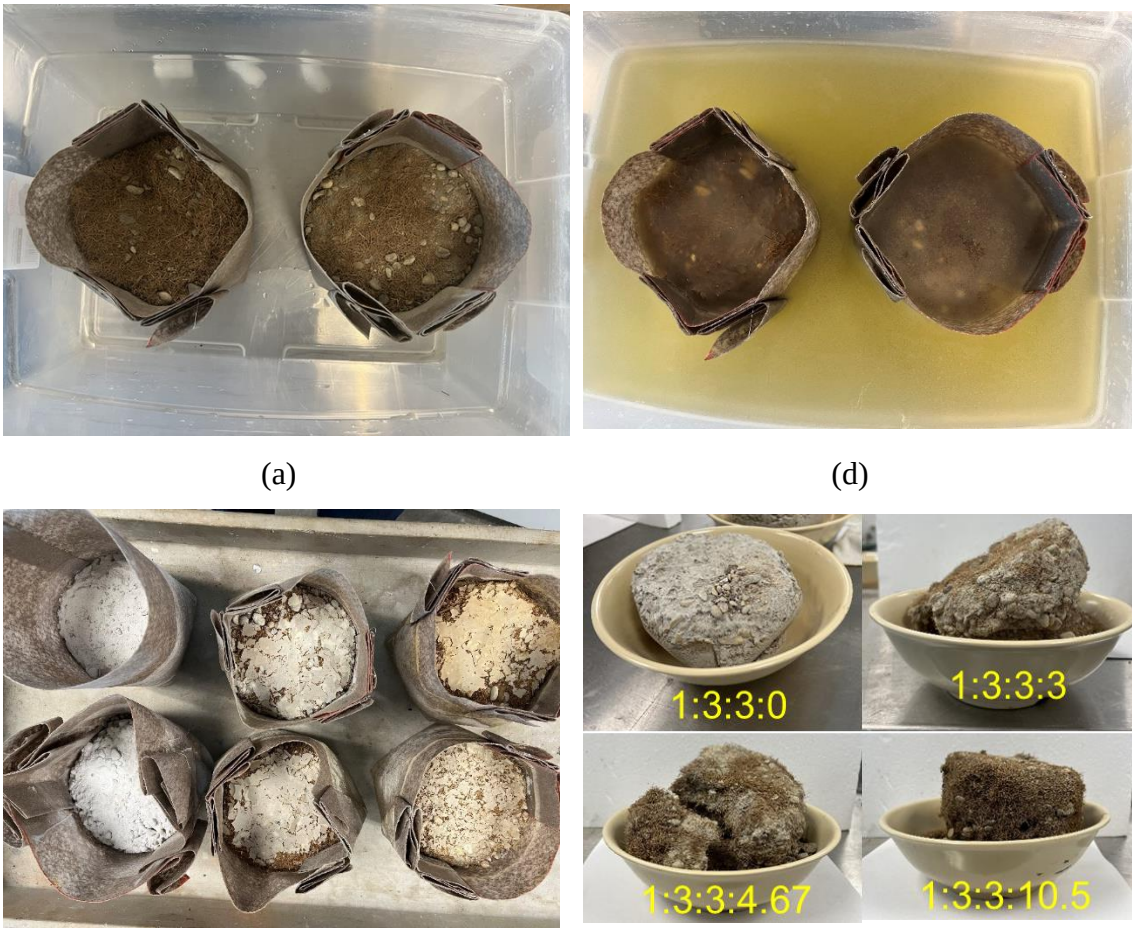

(a) (d)

(c) (d)

Figure 7. Small-scale wetting and drying tests (a) geotextile bags with the concrete mixture before the first wetting cycle, (b) bag during the wetting cycle, (c) sample during the drying cycle and (d) sample after 5 wetting and drying cycles

During the first wetting cycle, the dry mix was loosely placed to simulate the field applications and tested. The hydration process hardened the mixture. Subsequent wetting and drying cycles were conducted on the hardened concrete mixtures. After four drying cycles, the concrete mixtures were cured in drying conditions for an extended period before conducting the fifth wetting and drying cycle to evaluate the long-term durability of fiber-based concrete mixtures.

3.4.3.2. Large-Scale Tests

Large-scale wetting and drying tests were conducted on sand and one fiber-based concrete mixture. The mix 1:3:3:3 was chosen based on its durability properties to compare its performance against traditionally used sand. The large-scale wetting and drying studies were performed at room temperature in a large box with dimensions of 1.2 x 0.91 x 0.91 m, as shown in Figure 8a. Two channels with dimensions of 0.91 x 0.61 x 0.30 m were constructed within this large-scale box.

Two different sizes of bags were manufactured with the side faces made of nonwoven geotextile and the top and bottom faces made of thick textured cloth, providing friction resistance when the bags are stacked. Geotextile bags with dimensions of 0.30 x 0.30 x 0.10 m and 0.30 x 0.15 x 0.10 m were used in the current testing. The bags were filled using a pipe, slowly filling one set with sand and another set with dry fiber-based concrete mix. Once filled, the openings were glued with a glue gun, as shown in Figure 8b.

The stacking arrangement, as shown in Figure 8c, involved placing one bag of dimensions 0.30 x 0.30 x 0.10 m at the bottom, two bags of 0.30 x 0.15 x 0.10 m in the middle, and another bag of dimensions 0.30 x 0.30 x 0.10 m on top, forming a cube shape flood barrier in the middle of the channel creating a 0.30 x 0.30 x 0.30 m reservoir on both sides. This type of stacking was adopted to replicate the traditional sand-filled bag stacking in the field, where the sand-filled bags stacked at different levels experience different vertical stress and exhibit different wetting and drying properties.

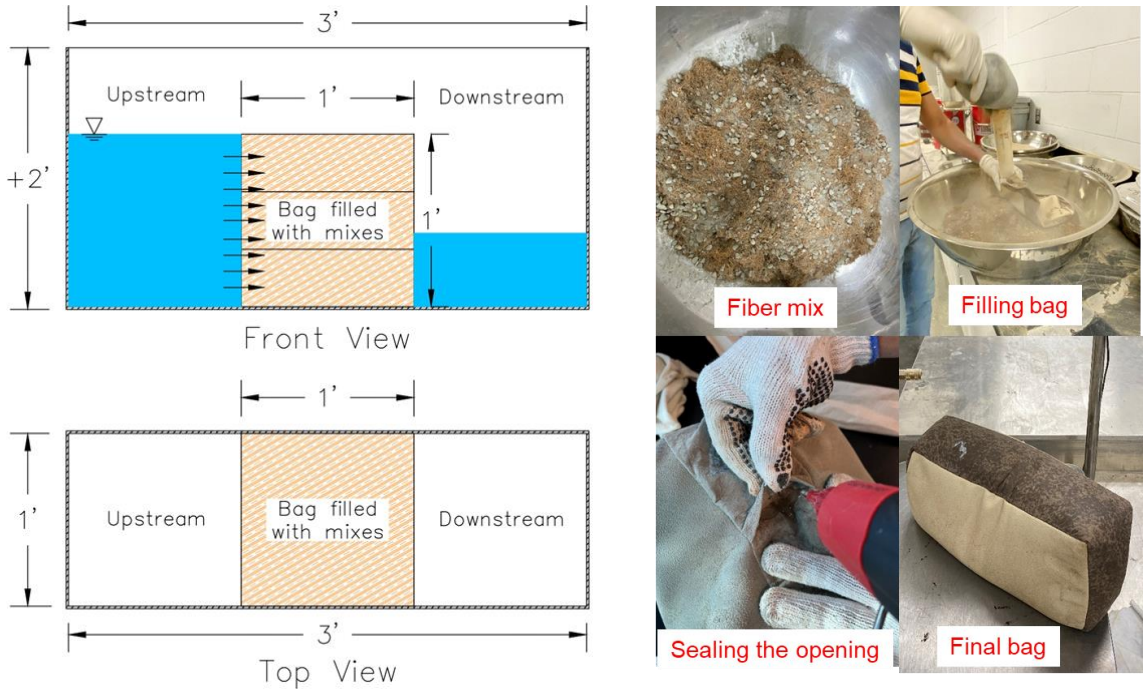

(a) (b)

(c)

Figure 8. Wetting and drying test Large-scale box: (a) Schematic diagram of large-scale box, (b) Steps involved in bag preparation, and (c) Large-scale box setup with stacked bags

Once the bags were placed in the box, wetting and drying tests were conducted on stacked bags at room temperature using potable water and saltwater. Two wetting and

drying cycles were conducted on each sample. The wetting cycle of the samples was conducted by filling one side of the stacked bags in the box, allowing the water to flow through the bag media to the other side until both sides reached a similar water head and were completely submerged. Weights were recorded for each bag every 24 hours until the sample reached a constant mass. After retrieving the bags from the water bath, the drying cycle was conducted by placing them in the large box again without any water at room temperature. Similar to the wetting cycle, the weights of the drying bag specimens were recorded every 24 hours until the weight change was negligible. In the current testing, any weight change of less than one percent over 24 hours was considered negligible, and the sample was assumed to have attained equilibrium.

During the first wetting cycle, the dry mixture bags were placed in the large box to simulate field applications and tested. The hydration process hardened the mix with 30% fibers due to the presence of cement. Subsequently, the second wetting and drying cycle was conducted on the hardened concrete mixture.

3.4.4. Strength Tests

In this study, traditional unconfined compressive strength tests and indirect tensile tests were performed to evaluate the strength properties of the fiber-based cement mixtures for potential future applications such as quick alternative semi-paved routes in emergency situations.

3.4.4.1. Unconfined Compressive Strength Test

The unconfined compressive strength (UCS) test was performed on 50 mm in diameter and 100 mm in height cylinder specimens. The duplicate cylindrical specimens were molded by placing the dry fiber-based cement mixture and allowing it to cure for 28 days in water at room temperature. The cured specimens were tested in the universal testing machine (UTM) in accordance with ASTM D2166 standard. The USC tests were performed using a 1% per minute strain rate until peak or specimen failure was observed. Figure 9a shows the UCS test being performed on a fiber-based cement mixture specimen.

3.4.4.2. Indirect Tensile Strength Test

The indirect tensile strength test was performed on the 150 mm diameter and 63.5 mm height cylinder specimens. Figure 9b shows the indirect tensile strength test setup.

(a) (b)

Figure 9 Strength tests' setup (a) Unconfined compressive strength test and (b) Indirect tensile strength test.

The duplicate cylindrical specimens were molded by placing the dry fiber-based cement mixture and allowing it to cure for 28 days in water at room temperature. The cured specimens were tested in the universal testing machine (UTM) in accordance with ASTM D6931. The specimens were loaded with a 1% strain per minute strain rate until failure was observed or 10% strain. The tensile strength of the fiber-based cement mixture was calculated using

$$S_t = \frac{2F}{\pi h d} \quad \textbf{(2)}$$

Where, S_t = Indirect tensile strength, MPa

F = Total applied vertical load at failure, N

h = Height of specimen, mm

d = Diameter of specimen, mm

Concrete with a cementitious mixture generally possesses brittle behavior, and stress-based testing is performed to evaluate its strength properties (compressive strength and split tensile strength). In stress-based testing, equal increment of load is applied over time until sample failure is observed. For brittle materials, failure is sudden and accompanied by a rapid drop in stress. However, for high fiber-based concrete mixtures, which are highly compressible and can withstand larger strains, strain-based testing is adopted. Stress-based testing is not suitable for fiber-based concrete mixtures because sudden changes in stress can result in very high strains, which will fail to capture the behavior of these mixtures accurately. Additionally, most construction materials used in civil engineering applications do not anticipate strains higher than 10%, so the testing was stopped at 10% and this was considered as failure in case of fiber-based concrete mixtures.

3.5. Testing Results

The current section discusses the experimental results obtained from various experimental tests conducted to understand the mechanical and durability behavior of fiber-based cement mixtures.

3.5.1. Free Swell Test

The free swell strain was performed on three fiber-based concrete mixtures to understand the mixture's swell behavior. Figure 10a shows the free swell strain vs elapsed time of the fiber-based concrete mixtures for mixture III (1:3:3:4.67), mixture II (1:3:3:7), and mixture I (1:3:3:10.5). Among the tested mixtures, mixture II showed the maximum free swell strain and mixture III showed the minimum free swell strain.

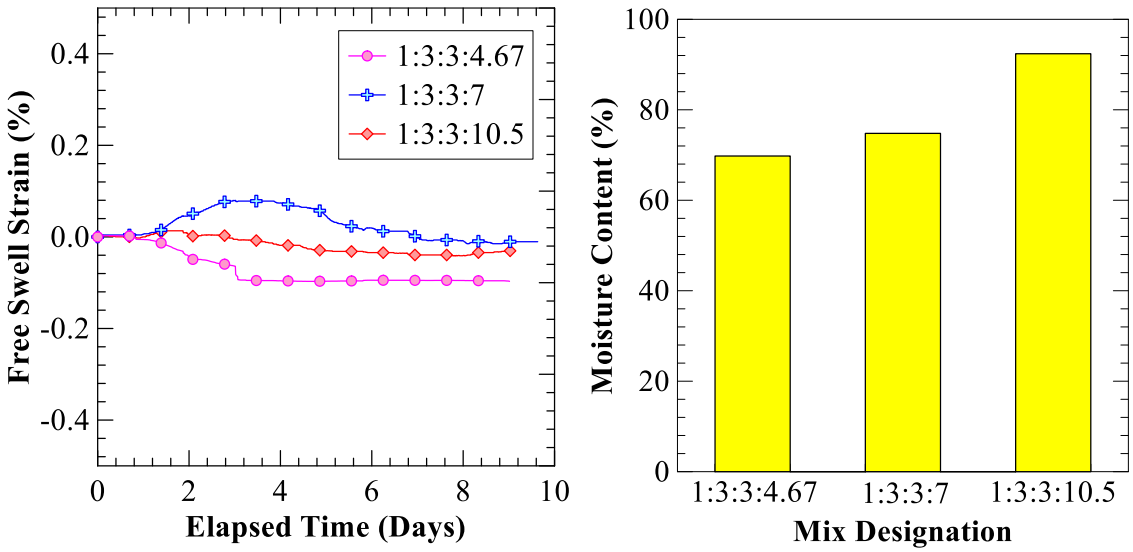

(a) (b)

Figure 10. Free swell testing results (a) Free swell strain vs elapsed time and (b) moisture content of the fiber-based concrete mixtures after free swell test

Mixture III experienced shrinkage strain as this mixture contained a high percentage of cement compared to the other two concrete mixtures. The hydration process in cement causes permanent volume shrinkage due to the exothermic chemical reaction when the cement phases react with the water. This could be the reason for mixture III experiencing shrinkage compared to other mixtures. After the test, mixture I had 92% water absorption compared to 70% and 75% water absorption in the case of mixture III and mixture II, respectively. This shows that the moisture absorption increased with an increase in the fiber content. The dry coir fibers are highly porous and the cellulose in fiber has numerous hydroxyl (–OH) groups that can form hydrogen bonds with water molecules, allowing the fibers to attract and hold moisture (Lin et al., 2017).

3.5.2. Permeability Studies

Figure 11 illustrates the coefficient of the permeability for various fiber-based concrete mixtures measured from falling head permeability tests. Among the five fiber-based concrete mixes, mixture V (1:3:3:0) exhibited the lowest permeability. Its permeability of 2.1×10^{-6} m/sec is comparable to pervious concrete materials (Qin et al., 2015), which typically range around 5×10^{-6} m/sec. The concrete mix has permeability compared to the

traditional concrete as the dry mixture is directly immersed in water which results in a high water/cement ratio. When the dry mixture combines with a high amount of water, more water is available to hydrate cement particles. However, the excess water that is not utilized in hydration fills the voids between cement particles and aggregates, forming interconnected capillary pores. These pores create a porous structure within the concrete, which allows water to penetrate more readily similar to pervious concrete.

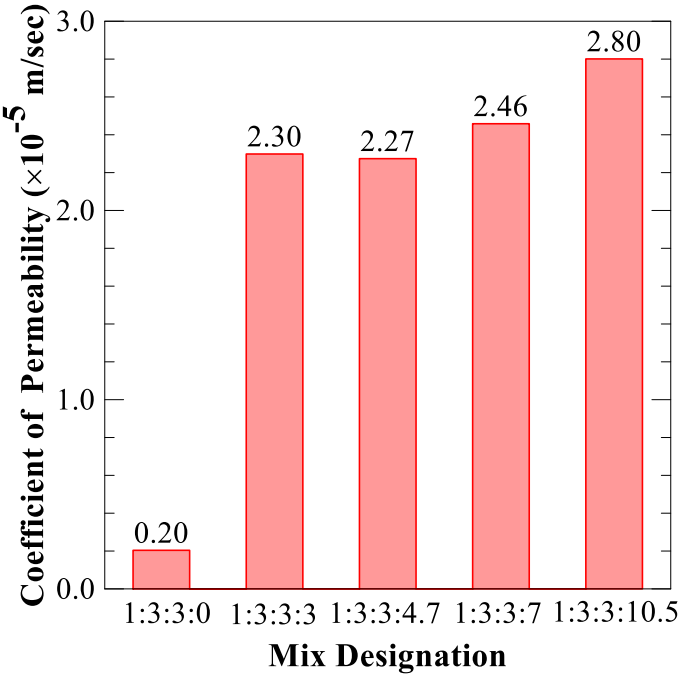

Figure 11. Coefficient of permeability for fiber-based concrete mixtures

The coefficient of permeability, *k*, for the concrete mixtures with fibers, varies from 2.1 × 10^{-5} m/sec to 2.8 × 10^{-5} m/sec, which falls within a similar range as sand permeability (Das & Sobhan, 2017). The results indicate that the incorporation of fibers into the concrete mixtures generally increased permeability compared to the mixture V, with higher fiber dosages correlating with higher permeability values. This phenomenon can be attributed to the presence of fibers creating larger voids within the concrete matrix. These voids, formed around and between the fibers, contribute to a more porous structure. As a result, water can pass through the concrete more easily, increasing its permeability.

3.5.3. Wetting and Drying Studies

3.5.3.1. Small Scale Tests

3.5.3.1.1. Potable water

Figure 12a to Figure 12c illustrates the cumulative water absorption and desorption over time for all three wetting and drying cycles of the fiber-based concrete mixtures tested at 4°C and 40% RH.

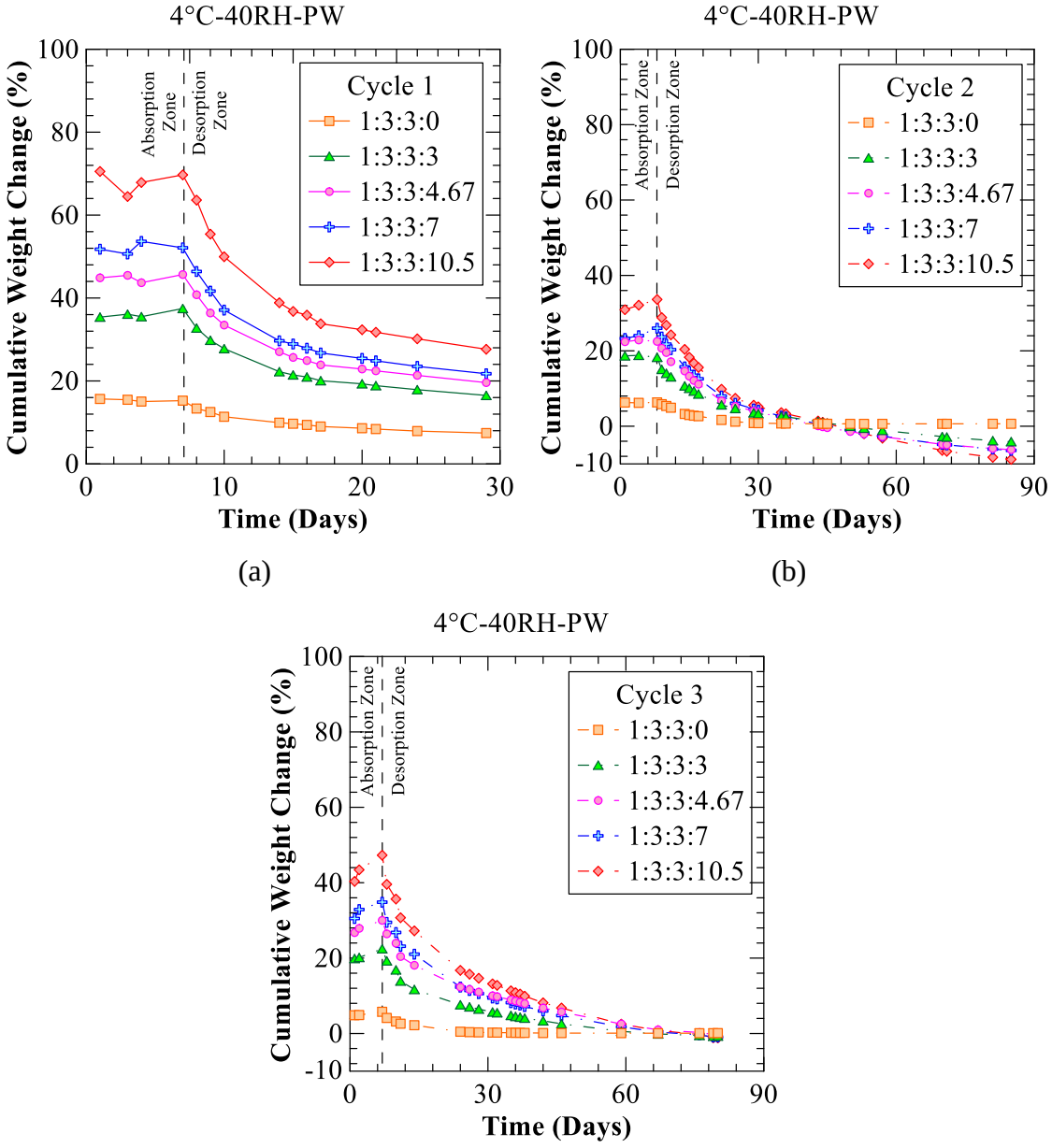

(c)

Figure 12. Graphs showing cumulative weight change vs time for fiber-based concrete mixtures tested at 4°C and 40% RH under potable water conditions (a) Cycle 1, (b) Cycle 2, (c) Cycle 3

Figure 13 shows the cumulative water absorption and desorption over time for all five wetting and drying cycles of the fiber-based concrete mixtures tested at 20°C and 50% RH. Figure 12 and Figure 13 illustrate that the cumulative change due to absorption remains almost constant for mixture V. In the case of the first absorption cycles, the control mix showed slightly more water absorption compared to the next four cycles in both testing environments. This might be due to the dry mix being used for the first wetting cycle, where the initial absorbed water starts the cement hydration and hardens the concrete mix. The hardened concrete mix holds water in the pores and allows more water to be absorbed resulting in decreased water absorption for subsequent cycles. Whereas in the case of concrete mixture I with 10.5 parts of fiber, the water absorption varied from one cycle to the next cycle. The change in water absorption trend from one cycle to the next cycle was not more than 10%.

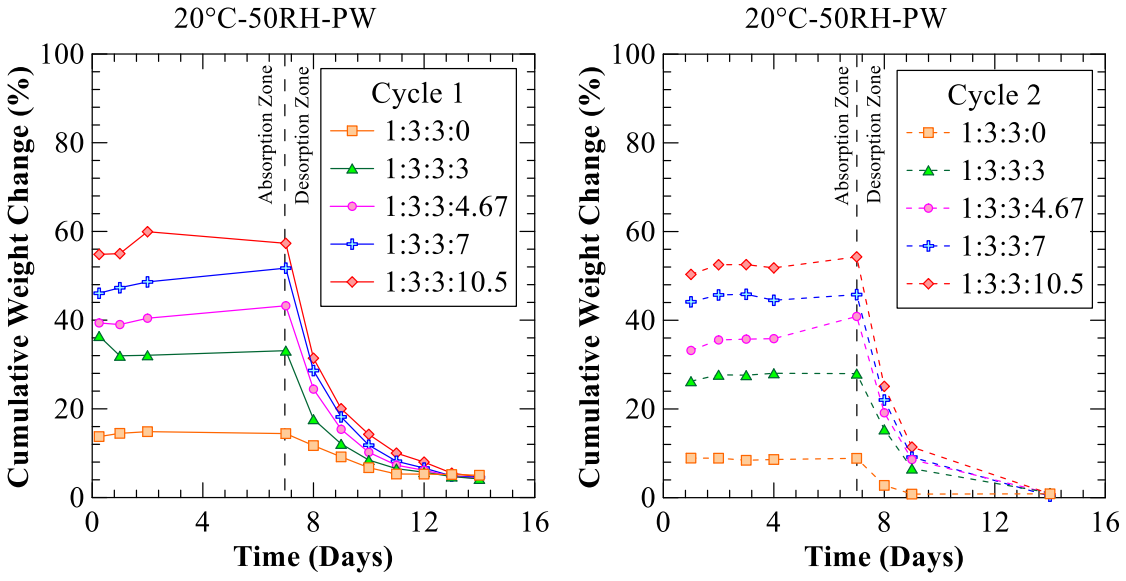

(a) (b)

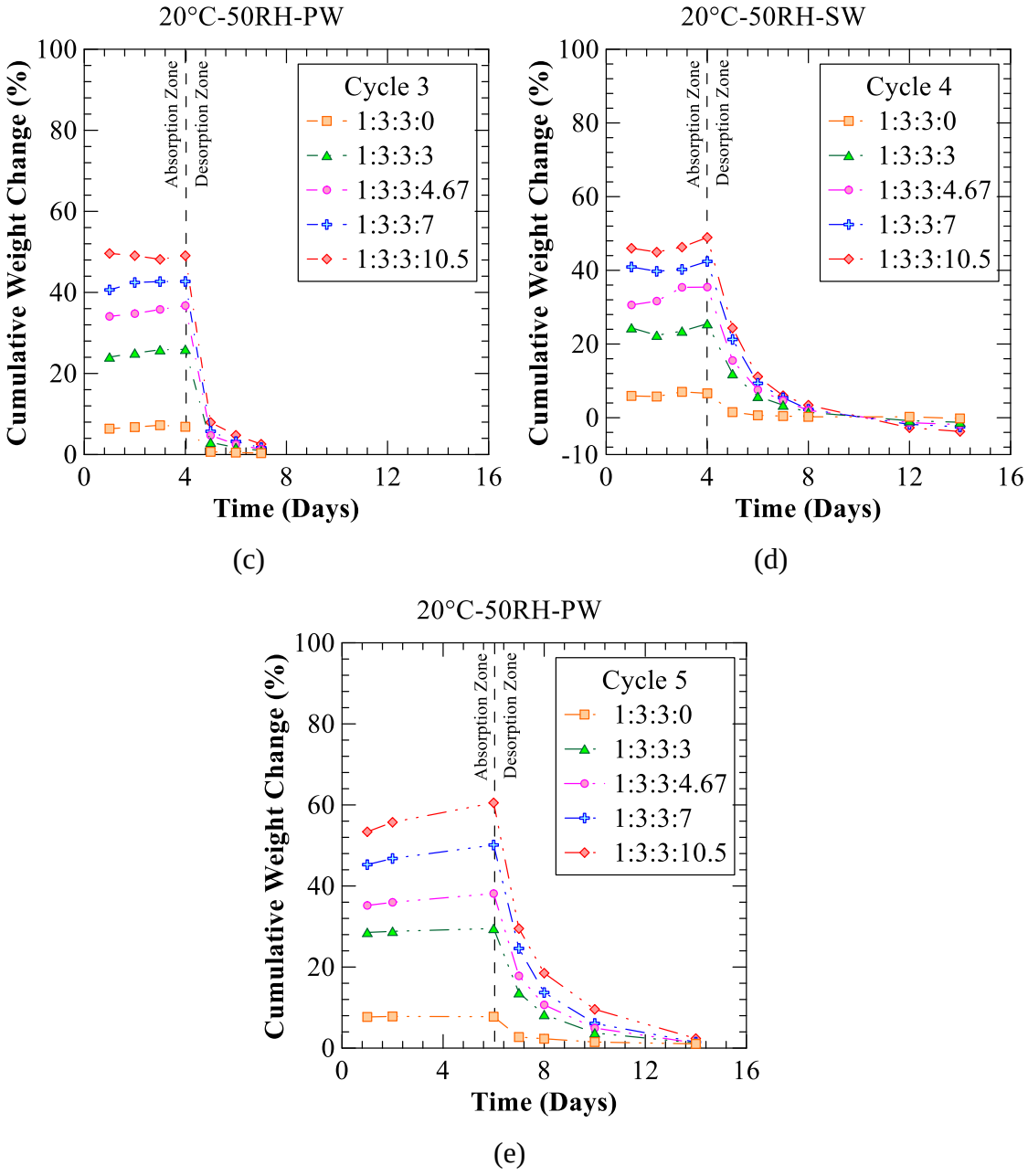

Figure 13. Graphs showing cumulative weight change vs time for fiber-based concrete mixtures tested at 20°C and 50% RH under potable water conditions (a) Cycle 1, (b) Cycle 2, (c) Cycle 3, (d) Cycle 4 and (e) Cycle 5

Figure 14 illustrates the cumulative water absorption and desorption over time for all five wetting and drying cycles of the fiber-based concrete mixtures tested at 40°C and 20% RH.

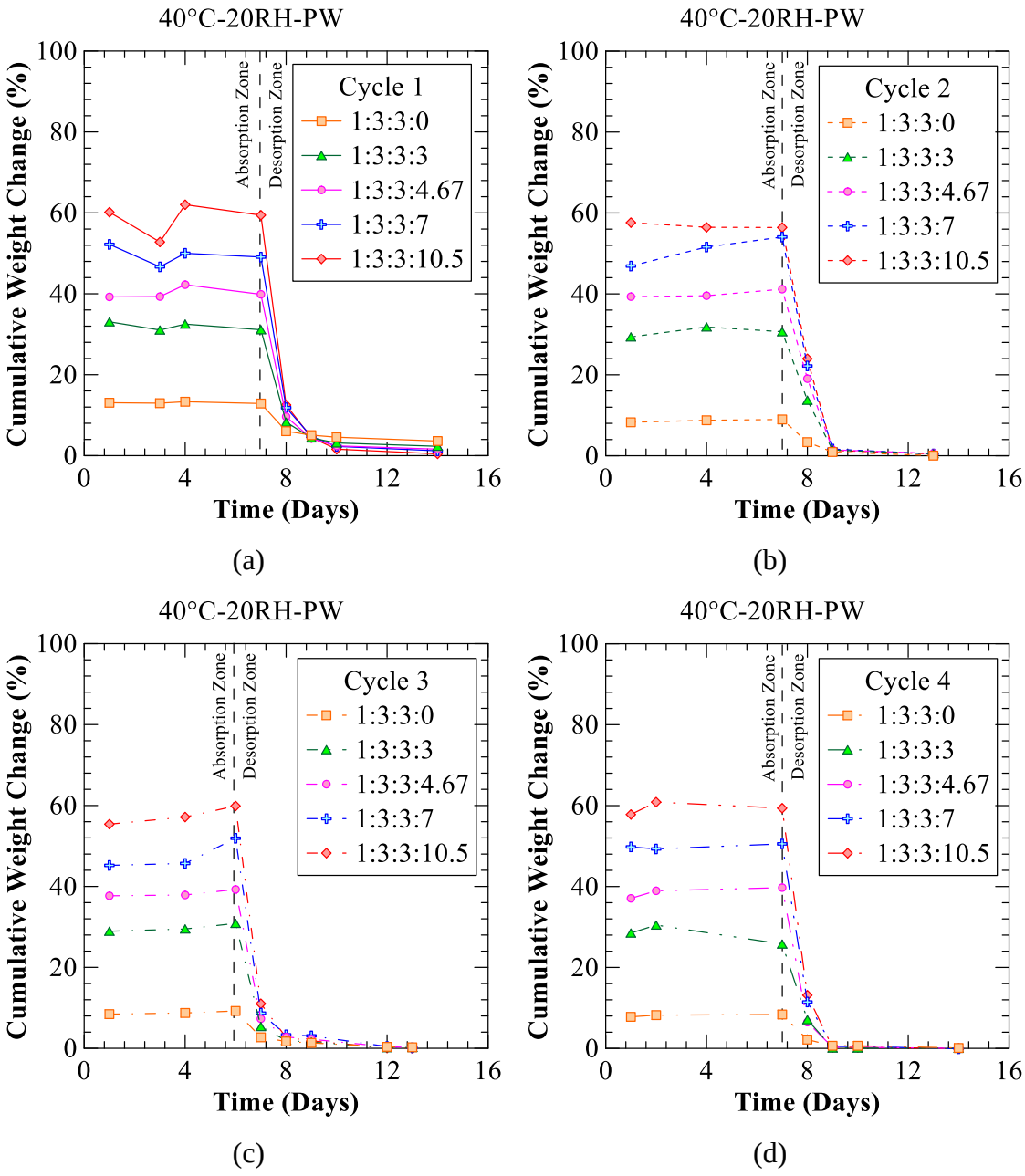
40°C-20RH-PW
Cumulative Weight Change (%)
Time (Days)
Absorption Zone
Desorption Zone
Cycle 1
1:3:3:0
1:3:3:3
1:3:3:4.67
1:3:3:7
1:3:3:10.5
(a)
40°C-20RH-PW
Cumulative Weight Change (%)
Time (Days)
Absorption Zone
Desorption Zone
Cycle 2
1:3:3:0
1:3:3:3
1:3:3:4.67
1:3:3:7
1:3:3:10.5
(b)
40°C-20RH-PW
Cumulative Weight Change (%)
Time (Days)
Absorption Zone
Desorption Zone
Cycle 3
1:3:3:0
1:3:3:3
1:3:3:4.67
1:3:3:7
1:3:3:10.5
(c)
40°C-20RH-PW
Cumulative Weight Change (%)
Time (Days)
Absorption Zone
Desorption Zone
Cycle 4
1:3:3:0
1:3:3:3
1:3:3:4.67
1:3:3:7
1:3:3:10.5
(d)

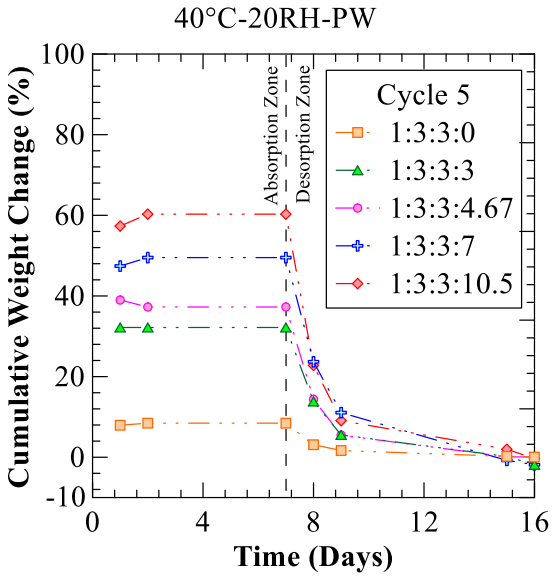

(e)

Figure 14. Graphs showing cumulative weight change vs time for fiber-based concrete mixtures tested at 40°C and 20% RH under potable water conditions (a) Cycle 1, (b) Cycle 2, (c) Cycle 3, (d) Cycle 4 and (e) Cycle 5

From Figure 12 to Figure 14, it can be observed that the concrete mixture I with 10.5 parts of fiber content has the highest water absorption, and mixture V poses the lowest water absorption. From these curves, a similar trend is found in all three testing conditions, as the fiber content in concrete increases the water absorption over time increases. The water absorption after 48 hours remained negligible for all concrete mixtures in three testing conditions indicating the system reached equilibrium. The mixes tested at 4°C showed slightly higher water absorption compared to specimens tested at 20°C and 40°C.

From Figure 12 to Figure 14, it can be observed that the fiber-based concrete mixture I with 10.5 parts of fiber content has the highest desorption, and mixture V with no fibers poses the lowest desorption. In all three testing environments, it is observed that desorption increases as the fiber dosage increases. Over time, all the concrete mixtures reached equilibrium i.e., the weight due to drying is negligible. Based on the testing environments, the time to reach equilibrium varied from 5 days to 70 days. In the case of 40 RH and 4°C, the specimens took 70 days to reach equilibrium whereas 5 days in 50 RH and 20°C, and 4 days in 20 RH and 40°C respectively. The variation is due to the

saturation gradient formed in the sample due to the temperature and relative humidity. As the temperature increases, the outer surface of the sample becomes dry, and the inner core of the sample stays wet creating a moisture gradient. In general tendency, the sample tries to attain equilibrium by releasing more water when a saturation gradient is formed making the desorption process quick in higher temperatures(Ramineni et al., 2024).

3.5.3.1.2. Saltwater

Figure 15 illustrates the cumulative weight change vs time for all five wetting and drying cycles of the fiber-based concrete mixtures tested with saltwater curing conditions. The wetting cycles for this set were performed at 4°C and 40% RH, while the drying cycles were accelerated by testing at 20°C and 50% RH. Similar to conditions with potable water, all the samples reached equilibrium within 2 days during all five wetting cycles. whereas, since the drying cycles at 20°C and 50% RH, the weight of the samples plateaued after 7 days of desorption.

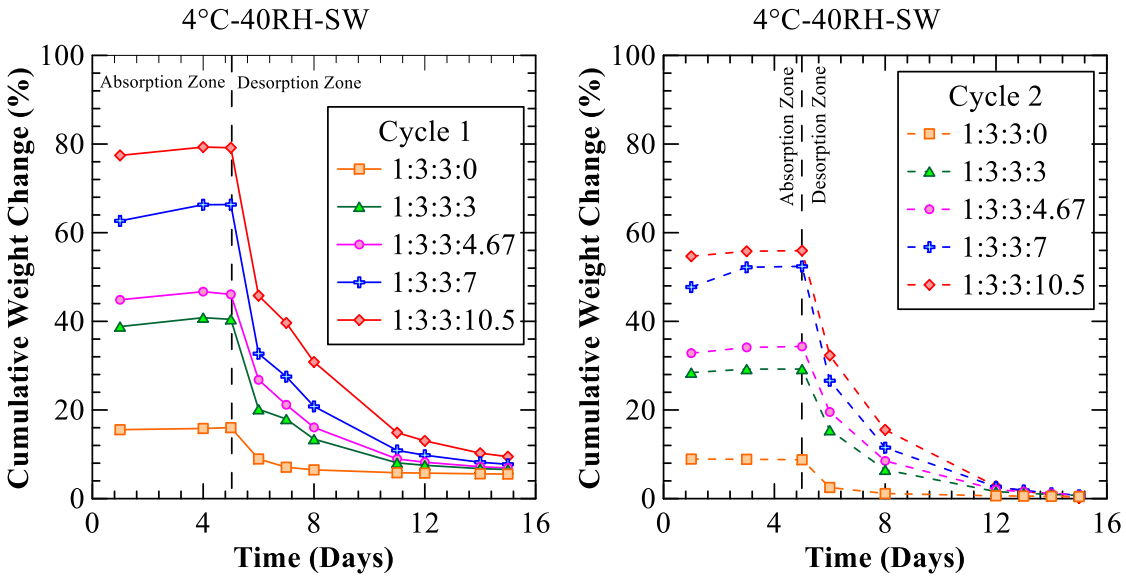

(a) (b)

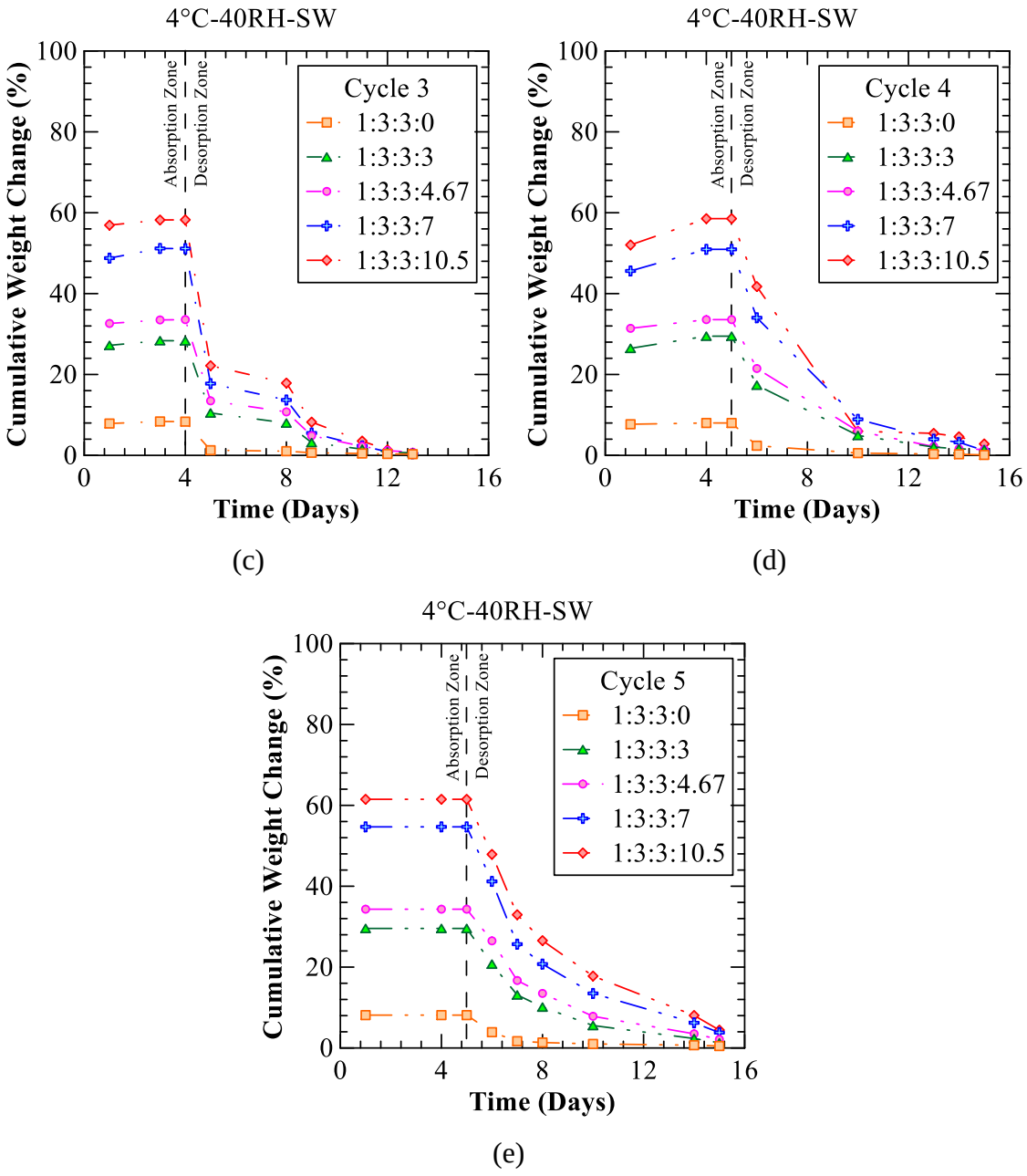

Figure 15. Graphs showing cumulative weight change vs time for fiber-based concrete mixtures tested at 4°C and 40% RH under saltwater conditions (a) Cycle 1, (b) Cycle 2, (c) Cycle 3, (d) Cycle 4 and (e) Cycle 5

Figure 16 shows the cumulative water absorption and desorption over time for all five wetting and drying cycles of the fiber-based concrete mixtures tested at 20°C and 50% RH.

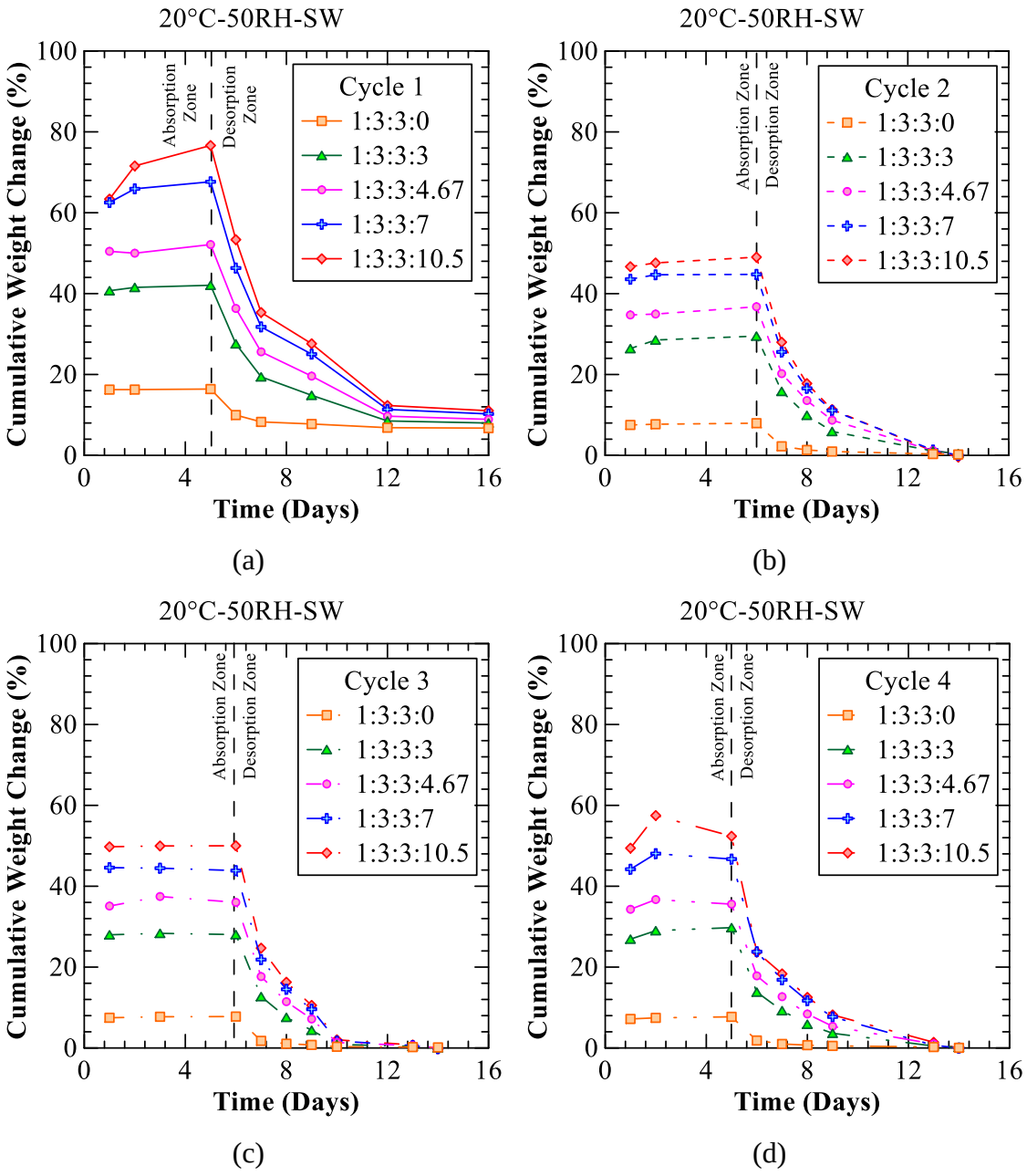
20°C-50RH-SW
Cumulative Weight Change (%)
Time (Days)
Absorption Zone
Desorption Zone
Cycle 1
1:3:3:0
1:3:3:3
1:3:3:4.67
1:3:3:7
1:3:3:10.5
(a)
20°C-50RH-SW
Cumulative Weight Change (%)
Time (Days)
Absorption Zone
Desorption Zone
Cycle 2
1:3:3:0
1:3:3:3
1:3:3:4.67
1:3:3:7
1:3:3:10.5
(b)
20°C-50RH-SW
Cumulative Weight Change (%)
Time (Days)
Absorption Zone
Desorption Zone
Cycle 3
1:3:3:0
1:3:3:3
1:3:3:4.67
1:3:3:7
1:3:3:10.5
(c)
20°C-50RH-SW
Cumulative Weight Change (%)
Time (Days)
Absorption Zone
Desorption Zone
Cycle 4
1:3:3:0
1:3:3:3
1:3:3:4.67
1:3:3:7
1:3:3:10.5
(d)

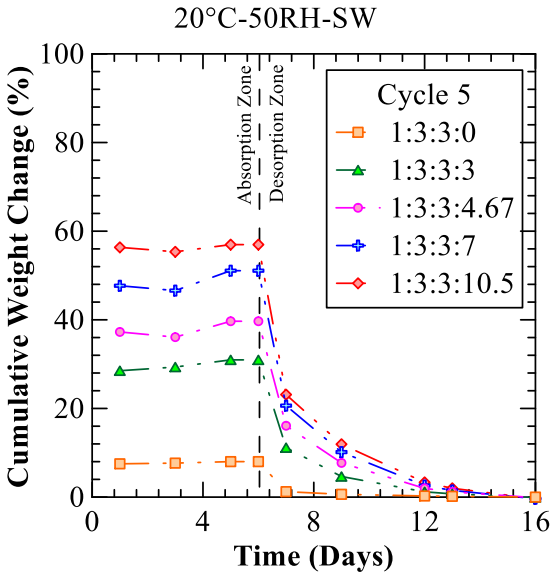

(e)

Figure 16. Graphs showing cumulative weight change vs time for fiber-based concrete mixtures tested at 20°C and 50% RH under saltwater conditions (a) Cycle 1, (b) Cycle 2, (c) Cycle 3, (d) Cycle 4 and (e) Cycle 5

From Figure 15 and Figure 16, it can be observed that the fiber-based concrete mixture I (1:3:3:10.5) exhibits the highest absorption and desorption, while the mixture V (1:3:3:0) shows the lowest absorption and desorption among the fiber-based concrete mixtures. Under saltwater conditions tested at 4°C and 40% RH, the 10.5 parts fiber mixture had over 80% absorption in the first cycle, which later dropped to 60% in subsequent cycles. A similar trend was observed in all other fiber-based concrete mixtures.

When the mixture I was tested at 20°C and 50% RH in potable water conditions, it reported slightly over 60% absorption in the first cycle, which dropped to 50% in subsequent cycles. In contrast, when tested at 20°C and 50% RH in saltwater, the same mixture reported 80% absorption in the first cycle, which later dropped to 60%, similar to the results at 4°C and 40% RH. This higher initial absorption in saltwater is due to the salt being absorbed into the samples, as salt tends to attract and retain more water.

In both saltwater and potable water testing environments, it was observed that absorption and desorption increased as the fiber dosage increased. The small-scale wetting

and drying results indicate that the fiber-based concrete samples exhibit closely similar absorption and desorption properties in both potable and saltwater conditions.

3.5.3.2. Large-Scale Tests

The results of large-scale wetting and drying tests conducted on natural sand and fiber-based concrete mixture IV (1:3:3:3) bags are illustrated in Figure 17 and Figure 18, respectively. Figure 17 shows the cumulative weight change due to wetting and drying cycle water over time for samples tested at room temperature under potable water conditions. Figure 17a and 17c represent the test results of cycle 1 and cycle 2, respectively, for the test on the natural sand, while Figure 17b and 17d represent the test results of cycle 1 and cycle 2, respectively, for the test on the fiber-based concrete mixture IV. Similarly, Figure 18 illustrates the cumulative weight change due to the wetting and drying cycle of water over time for saltwater conditions at room temperature.

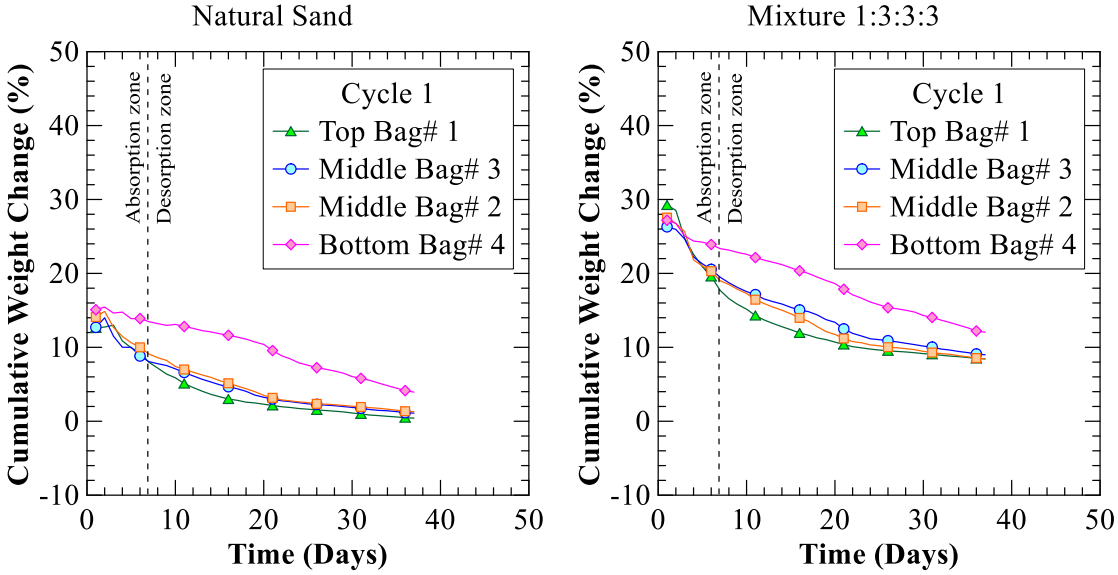

(a) (b)

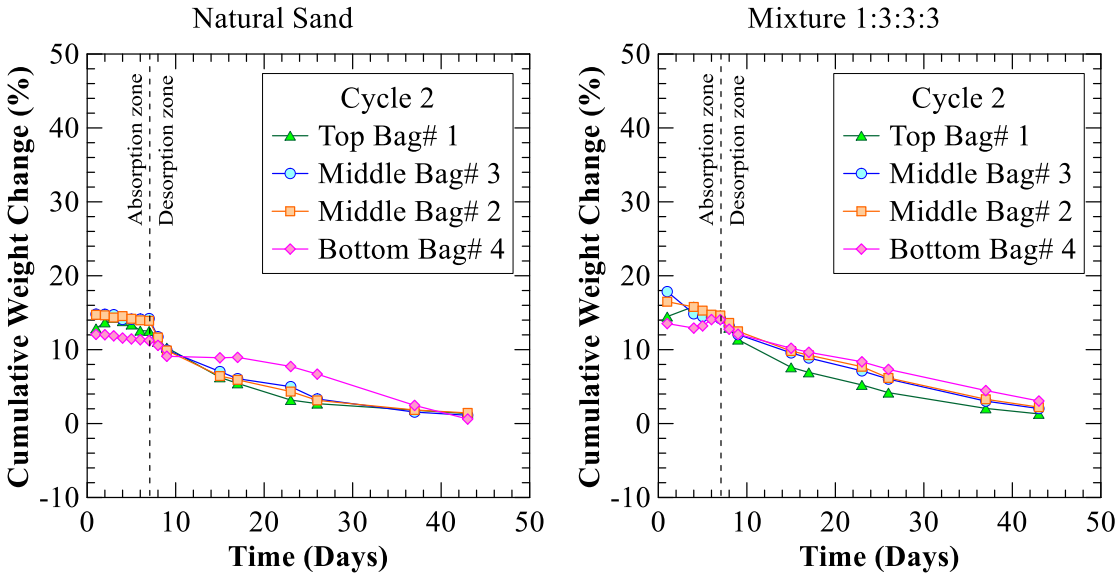

Figure 17. Results of weight change due to the wetting and drying cycle under potable water conditions: (a) Cycle 1 for natural sand, (b) Cycle 1 for mixture 1:3:3:3 (c) Cycle 2 for natural sand and (d) Cycle 2 for mixture 1:3:3:3

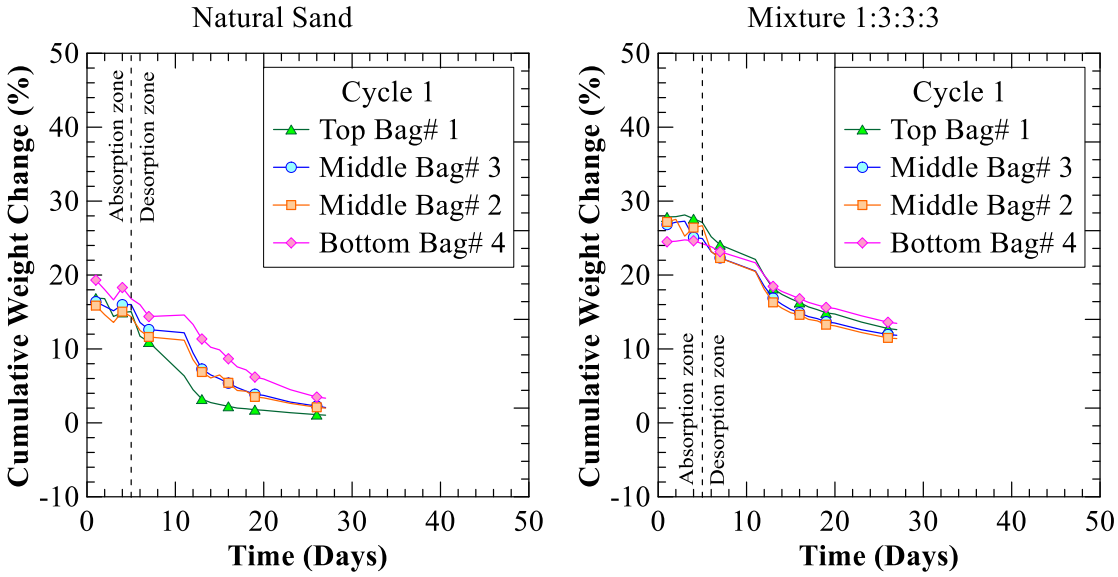

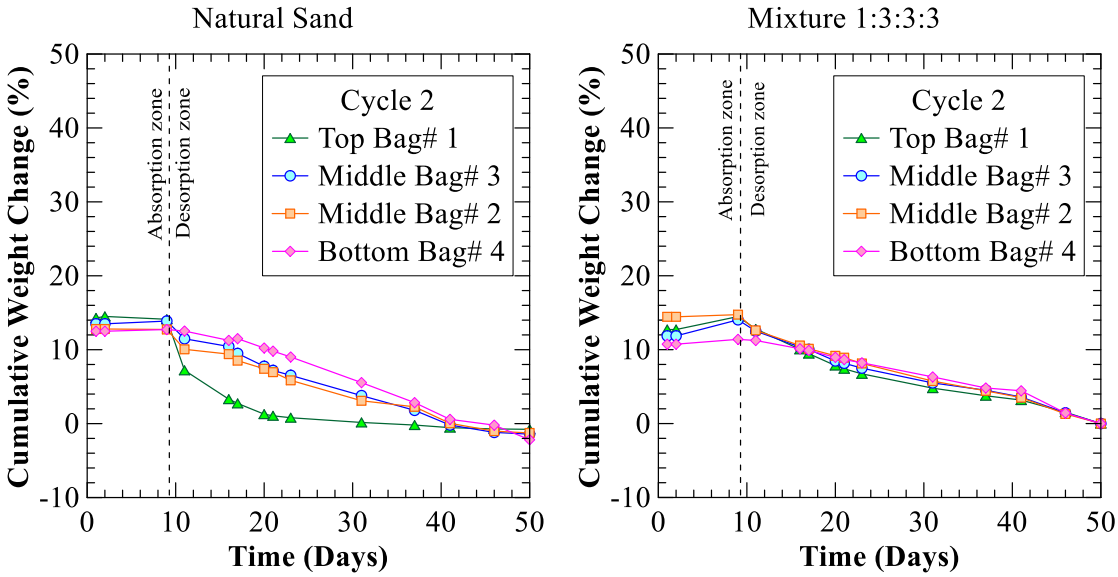

Figure 18. Results of weight change due to the wetting and drying cycle under saltwater conditions: (a) Cycle 1 for natural sand, (b) Cycle 1 for mixture IV (1:3:3:3) (c) Cycle 2 for natural sand and (d) Cycle 2 for mixture IV

In the initial testing, the flow rate of both natural sand and the concrete mixture was calculated by measuring the amount of water flow with respect to time from one end (upstream) through the bag media to the other end (downstream). It was noticed that the flow rate was 0.65 gal/min for natural sand and 0.21 gal/min for mixture IV. The natural sand showed a higher flow rate as compared to the mixture IV (1:3:3:3) due to the presence of sand only which has higher permeability. The presence of cement and fiber in mixture IV reduced the flow rate due to cement hardening leading to a drop in void and water absorption of fibers.

It can be observed in Figure 17 and Figure 18 that the fiber-based concrete mixture IV with 30% fiber content has a higher rate of cumulative weight change compared to the control mix due to the water absorption and desorption of fiber over the wetting and drying cycle. The results obtained generally show that in the drying cycle, bottom bag# 4 shows a higher rate of cumulative weight change compared to bags above due to a higher amount of entrapped moisture and a lower rate of evaporation of absorbed water from its body due to the lower exposure to the surrounding environment. The top and middle bags show

similar trends of lower cumulative weight change due to a higher rate of evaporation of absorbed water from its body due to more exposure to the surrounding environment where the top bag's surface is fully exposed to the environment. In both small-scale and large-scale wetting and drying tests, mixture IV showed similar weight change due to absorption and desorption in the first cycle and slightly lower weight change in the second cycle.

3.5.4. Strength Studies

3.5.4.1. Unconfined Compressive Strength

Figure 19a shows the compressive stress vs strain curves for the fiber-based concrete mixtures. All the fiber-based concrete mixtures except mixture V (1:3:3:0) experienced large strains under the vertical compressive stress as shown in Figure 11a indicating that the addition of fibers decreases the brittle behavior of the concrete mixture, which increases the compressibility of the concrete mixture. Figure 19b illustrates the USC of the fiber-based concrete mixtures corresponding to 10 % strain (except for mixture V which corresponds to failure strain).

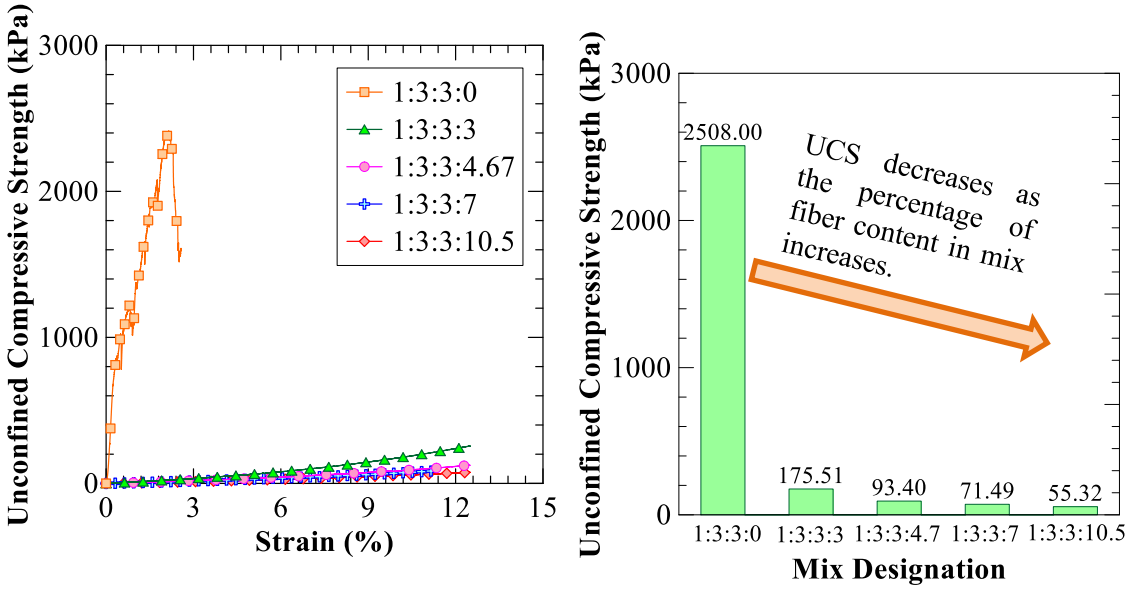

(a) (b)

Figure 19. Unconfined Compressive Strength (a) Stress vs strain curves and (b) UCS of fiber-based concrete mixtures.

As shown in Figure 19b, mixture V with no fiber content has the highest UCS, while mixture I with a ratio of 1:3:3:10.5 has the lowest UCS value among all the fiber-based concrete mixtures. The addition of fiber decreased the UCS value of the fiber-based concrete mixtures by 93 to 98% compared to the mixture V. This finding partially agrees with the past literature, which reported that an increase in fiber content beyond 2% of the volume of concrete decreases the compressive strength. However, most of the previous literature suggested that 1-2% fiber content is the optimum dosage to improve concrete strength properties (Ahmad et al., 2022; Martinelli et al., 2023). This study, however, used a minimum of 30% fiber content and a maximum of 60% fiber content, to understand the performance of high fiber dosage concrete mixtures.

3.5.4.2. Split Tensile Strength

Figure 20a shows the tensile stress vs strain curves of the fiber-based concrete mixture and Figure 20b illustrates the maximum indirect tensile strength of the fiber-based concrete mixtures. Similar to UCS results, all the fiber-based concrete mixtures except mixture V experienced large strains under compressive stress as shown in Figure 20a.

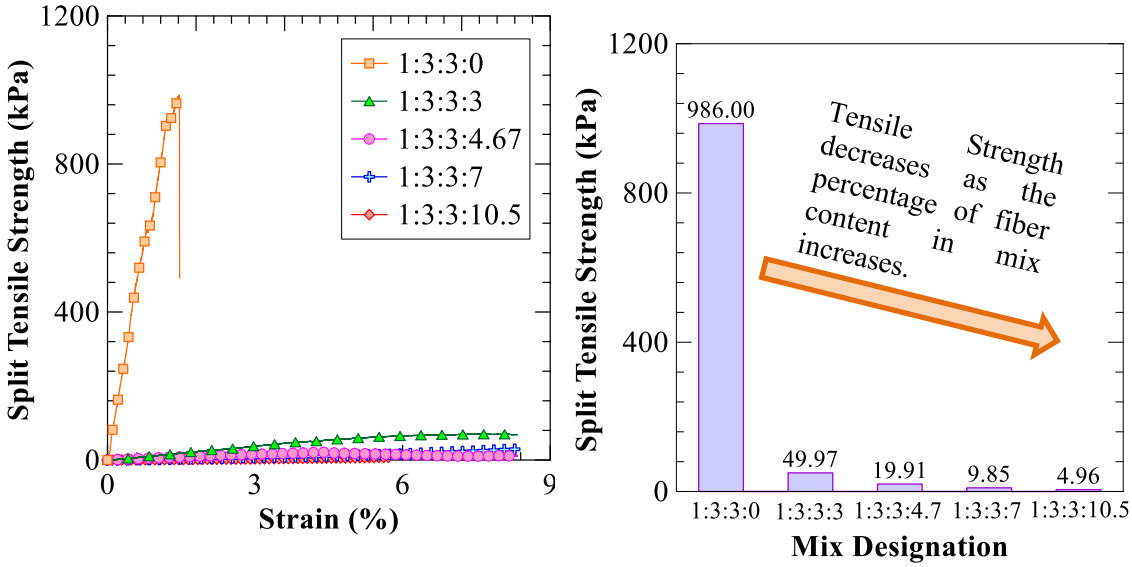

a) (b)

Figure 20. Split tensile strength (a) Stress vs strain curves and (b) Split tensile strength of fiber-based concrete mixtures

As shown in Figure 20b, the sudden failure of the 1:3:3:0 mix after reaching the peak indicates brittle failure, whereas the addition of fibers significantly improved the ductile behavior of the concrete mixtures. Mixture V recorded the highest split tensile strength of 985 kPa, while Mixture I recorded the lowest tensile strength of 4.96 kPa among the fiber-based concrete mixtures. The incorporation of fiber decreased the split tensile strength by 19 to 198 times compared to the mixture V. This shows that ductile behavior can be enhanced as the fiber dosage increases, and an increase in fiber dosage is inversely proportional to the strength of the sample.

There was ambiguity for using traditional strength tests for fiber based concrete mixtures, as the strength tests are developed for rigid materials and may not accurately assess the performance of high fiber-based concrete mixtures.

4. SUMMARY AND CONCLUSIONS

This study focused on developing fiber-based concrete mixes as an alternative material to replace sand-filled bags used as a flood barrier. The fiber dosage was optimized based on their free swell strain, permeability, water absorption/desorption and compressive and tensile strength properties. The following conclusions can be drawn from the experimental results:

1. Mixture II with 7 parts of fibers showed the maximum free swell strain, while mixture III with 4.67 parts of fibers exhibited shrinkage due to higher cement content, which causes permanent volume shrinkage during hydration.
2. The permeability of fiber-based concrete mixtures increased with higher fiber dosages. The presence of fibers created larger voids within the concrete matrix, resulting in a more porous structure and higher permeability.
3. The cumulative weight change due to absorption and desorption of the fiber-based concrete mixes increased as the fiber content increased.
4. Irrespective of the environment, the fiber-based concrete mixes reached equilibrium within 48 hours of absorption, and thereafter the weight change due to absorption remained negligible. In the case of desorption, the curing conditions, i.e. relative humidity and temperature, affected the rate of weight change due to drying.
5. The fiber-based concrete mixes showed slightly higher weight change in the first cycle and showed similar weight change trends due to absorption and desorption in the subsequent four cycles. This shows that fiber-based concrete mixes retain their water-holding and releasing capacity.
6. In both small-scale and large-scale wetting and drying tests, the mixture IV showed similar weight change due to absorption and desorption in the first cycle and slightly lower weight change in the second cycle.
7. The addition of fibers significantly reduced the unconfined compressive strength (UCS) and split tensile strength. Mixtures with higher fiber content experienced

large strains under stress, indicating improved ductile behavior but decreased strength compared to Mixture V.

Fiber-based concrete mixtures demonstrated promising results, particularly in terms of enhanced permeability and better absorption and desorption properties. However, these mixtures exhibit significantly lower compressive and tensile strength compared to no-fiber mixtures. Traditional strength tests are suitable for brittle materials and these tests fail to accurately capture the behavior of highly compressible fiber-based mixtures. This shows the need for developing reliable strength tests for these novel materials to accurately assess their performance and structural integrity. Despite the reduced strength, their high permeability and water absorption characteristics suggest that they could be viable alternatives to sandbags for flooding applications. Further studies are needed to optimize the fiber dosage and mix proportions to study the sustainability of these novel fiber-based concrete mixtures. Comprehensive feasibility assessments will help to better understand the potential of fiber-based concrete mixtures and their suitability for various flooding and erosion applications.

REFERENCES

Abdullah, A. (2011). Composite Cement Reinforced Coconut Fiber: Physical and Mechanical Properties and Fracture Behavior. In *Article in Australian Journal of Basic and Applied Sciences*. https://www.researchgate.net/publication/250310862

Ahmad, J., Majdi, A., Al-Fakih, A., Deifalla, A. F., Althoey, F., El Ouni, M. H., & El-Shorbagy, M. A. (2022). Mechanical and Durability Performance of Coconut Fiber Reinforced Concrete: A State-of-the-Art Review. In *Materials* (Vol. 15, Issue 10). MDPI. https://doi.org/10.3390/ma15103601

Ali, B., Hawreen, A., Ben Kahla, N., Talha Amir, M., Azab, M., & Raza, A. (2022). A critical review on the utilization of coir (coconut fiber) in cementitious materials. In *Construction and Building Materials* (Vol. 351). Elsevier Ltd. https://doi.org/10.1016/j.conbuildmat.2022.128957

Bradford, N. (2016). *Increases in Coastal Flooding*. Https://Www.Neefusa.Org/Nature/Land/Increases-Coastal-Flooding.

Das, B. M., & Sobhan, K. (2017). *Principles of Geotechnical Engineering (*9th ed.). Massachusetts: Cengage Learning.

Environmental Protection Agency. (2016). *Climate Change Indicators: Coastal Flooding*. Https://Www.Epa.Gov/Climate-Indicators/Climate-Change-Indicators-Coastal-Flooding.

EPA. (2023). *Climate Change Impacts on Coasts*.

Freeman, M. (2002). *Experiments and Analysis of Water-filled Tubes Used as Temporary Flood Barriers*. Virginia Polytechnic Institute and State University.

Gorman, M. T. (2020). *Design and Analysis of an Origami-Inspired and Hydrogel-Activated Flood Barrier*. University of Houston.

Hwang, C. L., Tran, V. A., Hong, J. W., & Hsieh, Y. C. (2016). Effects of short coconut fiber on the mechanical properties, plastic cracking behavior, and

impact resistance of cementitious composites. *Construction and Building Materials*, *127*, 984–992. https://doi.org/10.1016/j.conbuildmat.2016.09.118

Katman, H. Y. B., Khai, W. J., Bheel, N., Kırgız, M. S., Kumar, A., & Benjeddou, O. (2022). Fabrication and Characterization of Cement-Based Hybrid Concrete Containing Coir Fiber for Advancing Concrete Construction. *Buildings*, *12*(9). https://doi.org/10.3390/buildings12091450

Kevin Biggar, & Srboljub Masala. (1998). *Alternatives to sandbags for temporary flood protection*. https://publications.gc.ca/Collection/D82-46-1999E.pdf

Koňáková, D., Vejmelková, E., Čáchová, M., Siddique, J. A., Polozhiy, K., Reiterman, P., Keppert, M., & Černý, R. (2015). Treated Coconut Coir Pith as Component of Cementitious Materials. *Advances in Materials Science and Engineering*, *2015*. https://doi.org/10.1155/2015/264746

Lankenau, L., & Koppe, B. (2019). *Sandbagging versus Sandbag Replacement Systems: Costs, Time, Helpers, Logistics*. https://doi.org/doi.org/10.5194/nhess-2019-165

Lankenau, L., Massolle, C., Koppe, B., & Krull, V. (2020). Sandbag replacement systems – a nonsensical and costly alternative to sandbagging? *Natural Hazards and Earth System Sciences*, *20*(1), 197–220. https://doi.org/10.5194/nhess-20-197-2020

Lin, L., Fu, F., & Qin, L. (2017). Cellulose fiber-based high strength composites. In *Advanced High Strength Natural Fibre Composites in Construction* (pp. 179–203). Elsevier. https://doi.org/10.1016/B978-0-08-100411-1.00007-8

Martinelli, F. R. B., Ribeiro, F. R. C., Marvila, M. T., Monteiro, S. N., Filho, F. da C. G., & Azevedo, A. R. G. de. (2023). A Review of the Use of Coconut Fiber in Cement Composites. In *Polymers* (Vol. 15, Issue 5). MDPI. https://doi.org/10.3390/polym15051309

Massolle, C., Lankenau, L., & Koppe, B. (2018). Emergency Flood Control: Practice-Oriented Test Series for the Use of Sandbag Replacement Systems. *Geosciences*, *8*(12), 482. https://doi.org/10.3390/geosciences8120482

Meor, A., Fared, M., Meor, B., Mokhtar, R., Seyed, A., & Emamian, S. (2020). Impact of Coir Geotextiles to Reduce Soil Erosion and Surface Runoff. *Advances in Civil Engineering Materials*, 93–100. http://www.springer.com/series/15087

Mohammed, M., Jawad, A. J. afar M., Mohammed, A. M., Oleiwi, J. K., Adam, T., Osman, A. F., Dahham, O. S., Betar, B. O., Gopinath, S. C. B., & Jaafar, M. (2023). Challenges and advancement in water absorption of natural fiber-reinforced polymer composites. In *Polymer Testing* (Vol. 124). Elsevier Ltd. https://doi.org/10.1016/j.polymertesting.2023.108083

Qin, Y., Yang, H., Deng, Z., & He, J. (2015). Water Permeability of Pervious Concrete Is Dependent on the Applied Pressure and Testing Methods. *Advances in Materials Science and Engineering*, *2015*, 1–6. https://doi.org/10.1155/2015/404136

Ramineni, K., Congress, S. S. C., Biswas, N., Puppala, A. J., & Kriegstein, S. (2024, September 8). An Experimental Study to Evaluate the Performance of Fiber-Based Cement Mixture Bags as Alternative Flood and Erosion Barriers. *Geoenvironmeet*.

Ramli, M., Kwan, W. H., & Abas, N. F. (2013). Strength and durability of coconut-fiber-reinforced concrete in aggressive environments. *Construction and Building Materials*, *38*, 554–566. https://doi.org/10.1016/j.conbuildmat.2012.09.002

Rumbayan, R., & Ticoalu, A. (2019). *A study into flexural, compressive and tensile strength of coir-concrete as sustainable building material*. https://doi.org/10.1051/matecconf/20192

Teixeira, R. S., Bufalino, L., Denzin Tonoli, G. H., dos Santos, S. F., & Savastano Junior, H. (2022). Coir fiber as reinforcement in cement-based materials. In *Advances in Bio-Based Fiber* (pp. 707–739). Elsevier. https://doi.org/10.1016/B978-0-12-824543-9.00008-6

US Army Corps of Engineers. (2012). *Flood Fighting Techniques*.

Wang, L., Cui, S., Li, Y., Huang, H., Manandhar, B., Nitivattananon, V., Fang, X., & Huang, W. (2022). A review of the flood management: from flood control to flood resilience. In *Heliyon* (Vol. 8, Issue 11). Elsevier Ltd. https://doi.org/10.1016/j.heliyon.2022.e11763

Wuebbles, D. J., Fahey, D. W., & Hibbard, K. A. (2017). *Climate Science Special Report: Fourth National Climate Assessment*. https://doi.org/10.7930/J0J964J6